Modelling the optical polarized emission of AR Scorpii white dwarf pulsar

Fidy A. Ramamonjisoa
(in collaboration with P.J. Meintjes (UFS), S.B. Potter (SAAO), D.A.H. Buckley (SAAO), K.K. Singh (BARC))

Department of Physics
University of the Free State, South Africa

April 14, 2021

Outline

AR Sco properties

- White dwarf (WD):
  - $M_{\rm WD} = 0.8 M_{\odot}$, highly magnetic $\sim$ few hundred MG **(Buckley et al. 2017)**
  - **Spin period: 117 s**

AR Sco properties

- White dwarf (WD):
  - $M_{\rm WD} = 0.8 M_{\odot}$, highly magnetic $\sim$ few hundred MG **(Buckley et al. 2017)**
  - **Spin period: 117 s**
- M5-type dwarf (MD):
  - $M_{\rm MD} = 0.3 M_{\odot}$
  - **Orbital period: 3.56 hr**

AR Sco properties

- White dwarf (WD):
  - $M_{\rm WD} = 0.8 M_{\odot}$, highly magnetic $\sim$ few hundred MG **(Buckley et al. 2017)**
  - **Spin period: 117 s**
- M5-type dwarf (MD):
  - $M_{\rm MD} = 0.3 M_{\odot}$
  - **Orbital period: 3.56 hr**
- AR Sco exhibits pulsed emission from radio to UV/X-ray **(Marsh et al. 2016)**

AR Sco properties

- White dwarf (WD):
  - $M_{\rm WD} = 0.8 M_{\odot}$, highly magnetic $\sim$ few hundred MG **(Buckley et al. 2017)**
  - **Spin period: 117 s**
- M5-type dwarf (MD):
  - $M_{\rm MD} = 0.3 M_{\odot}$
  - **Orbital period: 3.56 hr**
- AR Sco exhibits pulsed emission from radio to UV/X-ray **(Marsh et al. 2016)**
- The spectral energy distribution (SED) in optical to X-ray suggest a strong synchrotron component **(Marsh et al. 2016)**

AR Sco properties

- White dwarf (WD):
  - $M_{\rm WD} = 0.8 M_{\odot}$, highly magnetic $\sim$ few hundred MG **(Buckley et al. 2017)**
  - **Spin period: 117 s**
- M5-type dwarf (MD):
  - $M_{\rm MD} = 0.3 M_{\odot}$
  - **Orbital period: 3.56 hr**
- AR Sco exhibits pulsed emission from radio to UV/X-ray **(Marsh et al. 2016)**
- The spectral energy distribution (SED) in optical to X-ray suggest a strong synchrotron component **(Marsh et al. 2016)**
- Linear polarization degree $\sim$ **40% (Buckley et al. 2017)**

AR Sco properties

- White dwarf (WD):
  - $M_{\rm WD} = 0.8 M_{\odot}$, highly magnetic $\sim$ few hundred MG **(Buckley et al. 2017)**
  - **Spin period: 117 s**
- M5-type dwarf (MD):
  - $M_{\rm MD} = 0.3 M_{\odot}$
  - **Orbital period: 3.56 hr**
- AR Sco exhibits pulsed emission from radio to UV/X-ray **(Marsh et al. 2016)**
- The spectral energy distribution (SED) in optical to X-ray suggest a strong synchrotron component **(Marsh et al. 2016)**
- Linear polarization degree $\sim$ **40% (Buckley et al. 2017)**
- Linearly polarized emission is modulated on both the spin period of the WD and **beat period (1.97 min)** between the spin and orbital periods **Marsh et al. (2016)**, **Buckley et al. (2017)**, **Potter and Buckley (2018)**

AR Sco properties

- White dwarf (WD):
  - $M_{\rm WD} = 0.8 M_{\odot}$, highly magnetic $\sim$ few hundred MG **(Buckley et al. 2017)**
  - **Spin period: 117 s**
- M5-type dwarf (MD):
  - $M_{\rm MD} = 0.3 M_{\odot}$
  - **Orbital period: 3.56 hr**
- AR Sco exhibits pulsed emission from radio to UV/X-ray **(Marsh et al. 2016)**
- The spectral energy distribution (SED) in optical to X-ray suggest a strong synchrotron component **(Marsh et al. 2016)**
- Linear polarization degree $\sim$ **40% (Buckley et al. 2017)**
- Linearly polarized emission is modulated on both the spin period of the WD and **beat period (1.97 min)** between the spin and orbital periods **Marsh et al. (2016)**, **Buckley et al. (2017)**, **Potter and Buckley (2018)**
- No evident sign of accretion **(Marsh et al. 2016)**

Photopolarimetric observations

- Instrument: HIgh-speed-Photo-POlarimeter (HIPPO)
- South African Astronomical Observatory (SAAO) 1.9 m telescope

Table: Observations used to constrain the model **(Potter and Buckley 2018)**

Date	Duration (h)	Filters
14 May 2016	5.60	Clear
25 May 2016	4.70	OG570, clear
26 May 2016	7.37	OG570, clear
27 May 2016	6.82	OG570, clear
27 Mars 2017	4.03	Clear
28 Mars 2017	4.07	Clear

Emission scenarios of AR Sco

- Rotating Vector Model (RVM) (emission regions located near the magnetic poles of WD) **(du Plessis et al. 2019)**
- Model of synchrotron emission produced by electrons trapped at the magnetosphere of WD and accelerated to the magnetic mirror points **(Potter and Buckley 2018)**
- Synchrotron emission model produced at magnetic mirror points of the electron motion **(Takata and Cheng 2019)**
- Striped pulsar wind model outside the light cylinder for oblique rotator **(Ramamonjisoa et al. 2021 in preparation)**

The striped pulsar wind model

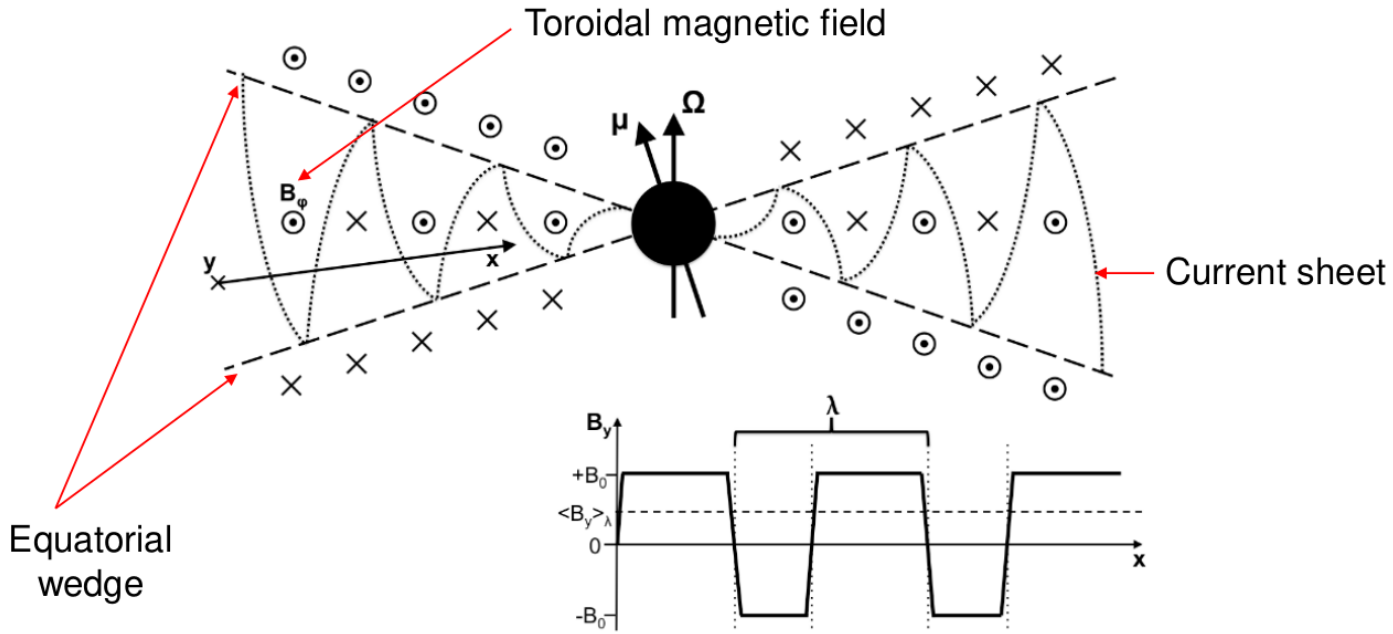

Figure: Toroidal stripes with alternating polarity **(Lorenzo et al. 2012)**

Physical length of the current sheet:

$$\sim 2\pi\beta r_{\rm L}/\Delta \tag{1}$$

Magnetic field based on asymptotic solution (Bogovalov 1999)

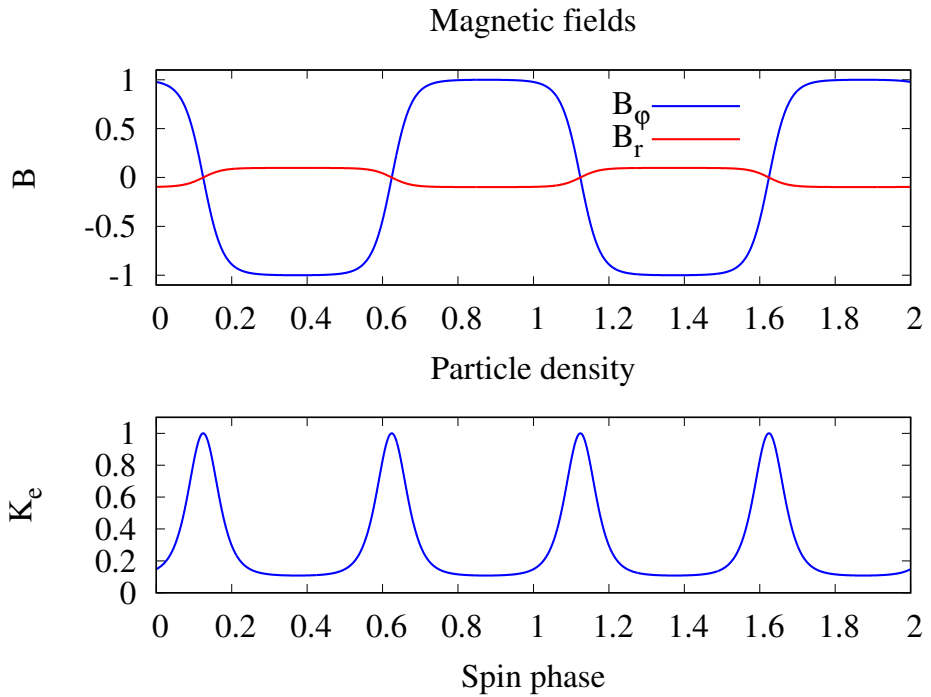

Figure: The magnetic fields and particle density profiles (Pétri 2013)

$$\boldsymbol{B} = \beta^2 B_{\rm L} \left(\frac{r_{\rm L}}{r}\right)^2 \tanh(\psi/\Delta)\boldsymbol{e}_{\rm r} - \beta B_{\rm L}\left(\frac{r_{\rm L}}{r}\right)\sin\theta\tanh(\psi/\Delta)\boldsymbol{e}_{\varphi} \qquad (2)$$

$$K_{\rm e}(\boldsymbol{r},t) = \frac{N_{\rm c}\tanh^2(\psi/\Delta)}{r^2} + \frac{N_{\rm h}(1-\tanh^2(\psi/\Delta))}{r^2} \qquad (3)$$

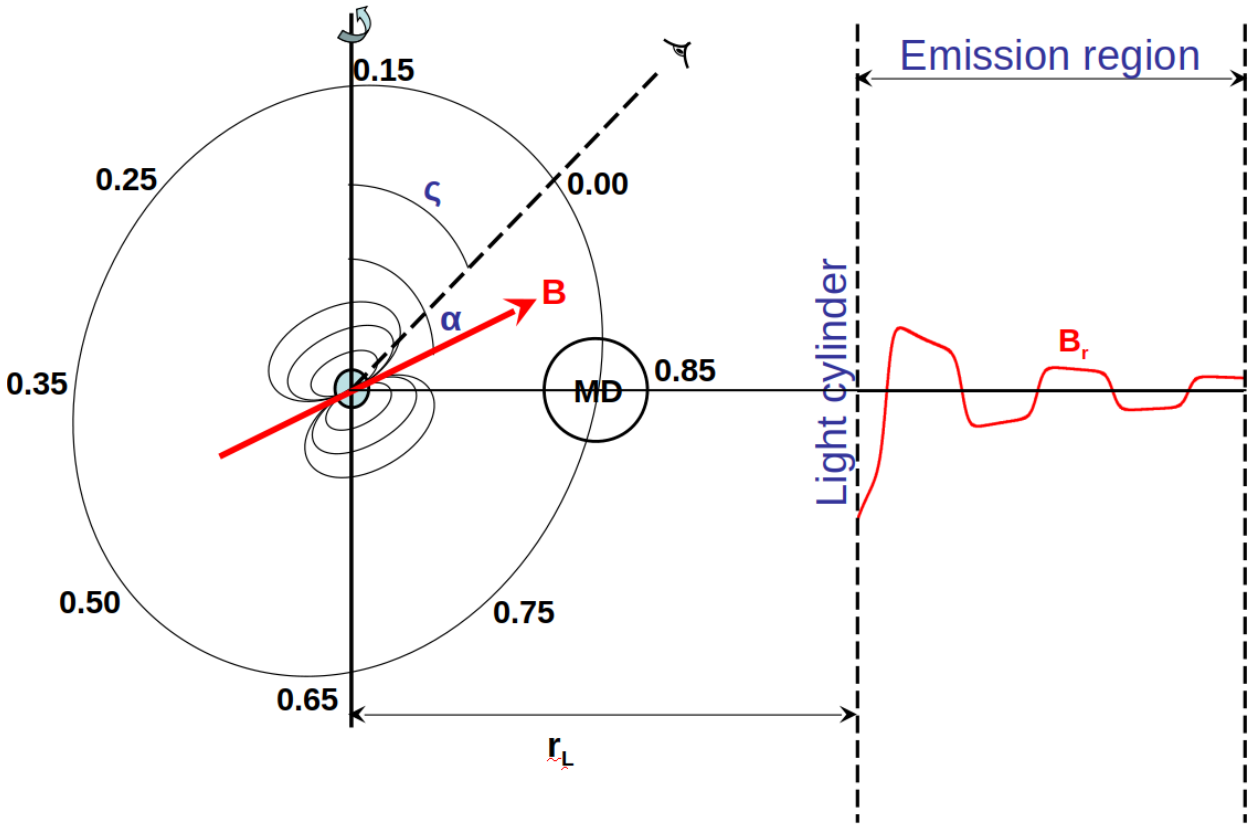

Figure: The decreasing radial component of the magnetic field (not to scale).

The Stokes parameters

Lyutikov et al. (2003), Pétri (2013)

$$
\begin{aligned}
I_\omega(t_{\rm obs}) &= \int_{V_{\rm wind}} s_0(\mathbf{r}, t_{\rm ret}) \frac{p+7/3}{p+1} dV, \\
Q_\omega(t_{\rm obs}) &= \int_{V_{\rm wind}} s_0(\mathbf{r}, t_{\rm ret}) \cos(2\chi) dV, \\
U_\omega(t_{\rm obs}) &= \int_{V_{\rm wind}} s_0(\mathbf{r}, t_{\rm ret}) \sin(2\chi) dV. \qquad (4)
\end{aligned}
$$

Retarded time: (5)

$$
t_{\rm ret} = t_{\rm obs} + \frac{\boldsymbol{n}\cdot\boldsymbol{r}}{c}. \qquad (6)
$$

$$
s_0(\mathbf{r}, t) = \kappa K_{\rm e}(\mathbf{r}, t) \omega^{\frac{1-p}{2}} \mathcal{D}^{\frac{p+3}{2}} \left(\frac{B}{\Gamma} \sqrt{1 - (\mathcal{D}\boldsymbol{n}\cdot\boldsymbol{b})^2} \right)^{(p+1)/2} \qquad (7)
$$

The magnetic field and particle density

$$\kappa = \frac{\sqrt{3}}{8\pi}\Gamma_{\rm E}\left(\frac{3p-1}{12}\right)\Gamma_{\rm E}\left(\frac{3p+7}{12}\right)\frac{e^3}{4\pi\epsilon_0 m_{\rm e} c}\left(\frac{3e}{m_{\rm e}^3 c^4}\right)^{(p-1)/2} \tag{8}$$

Doppler boosting factor:

$$\mathcal{D} = \frac{1}{\Gamma(1-\boldsymbol{n}\cdot\boldsymbol{v}/c)}. \tag{9}$$

Current sheet is defined by the surface $\psi \sim 0$ where:

$$\psi = \cos\theta\cos\alpha + \sin\theta\sin\alpha\cos[\varphi - \Omega(t - r/v)]. \tag{10}$$

Simulation

Table: Definition of the physical parameters used in the model.

Name	Symbol
Inner radius of the emission	r_0
Outer radius of the emission	$r_{\max}$
Particle energy index	p
Inclination of the line of sight (LOS)	ζ
Obliquity of the magnetic field	α
Bulk Lorentz factor of the wind	Γ
Particle density contrast	K_0
Current sheet thickness	Δ

Magnetic field strength at the surface of light cylinder

$$B_{\rm L} = \sqrt{\frac{L_{\rm WD}}{c r_{\rm L}}} \simeq \mathbf{0.3}\ \mathrm{G},\ \textbf{(Lyubarsky 2003)} \tag{11}$$

with $L_{\rm WD} = 1.3 \times 10^{25}\ \mathrm{W}$ and $r_{\rm L} \simeq 6 \times 10^{11}\ \mathrm{cm}$.

$$r_{\rm max} = \left(\frac{\pi \omega_{\rm L}}{2\Omega}\right) r_{\rm L}, \tag{12}$$

where Ω is the angular velocity of WD,
$\omega_{\rm L}$ is the gyrofrequency at the light cylinder:

$$\omega_{\rm L} = \frac{e B_{\rm L}}{m_e c}. \tag{13}$$

Outer radius of emission

$$r_{\rm max} \simeq 10^8 r_{\rm L}$$

Predicted value of the wind Lorentz factor Γ

$$\Gamma = 10\ \tau_{\rm rec}^{1/5} \sqrt{\frac{L_{\rm sd}}{10^{28}\ {\rm W}}}, \quad \textbf{(Pétri 2012)} \tag{14}$$

where $L_{\rm sd}$ is the spin-down power of the white dwarf, $\tau_{\rm rec}$ is the **reconnection rate**:

$$\tau_{\rm rec} \simeq 0.5 \left(\frac{L_{\rm sd}}{10^{28}\ {\rm W}} \right)^{-5/12}. \tag{15}$$

The **rate of energy loss** of the white dwarf is:

$$L_{\rm sd} = -4\pi^2 I \nu_{\rm WD}\ \dot{\nu}_{\rm WD}. \tag{16}$$

We find a bulk Lorentz factor: $\Gamma \simeq 1.5$.

Numerical simulation

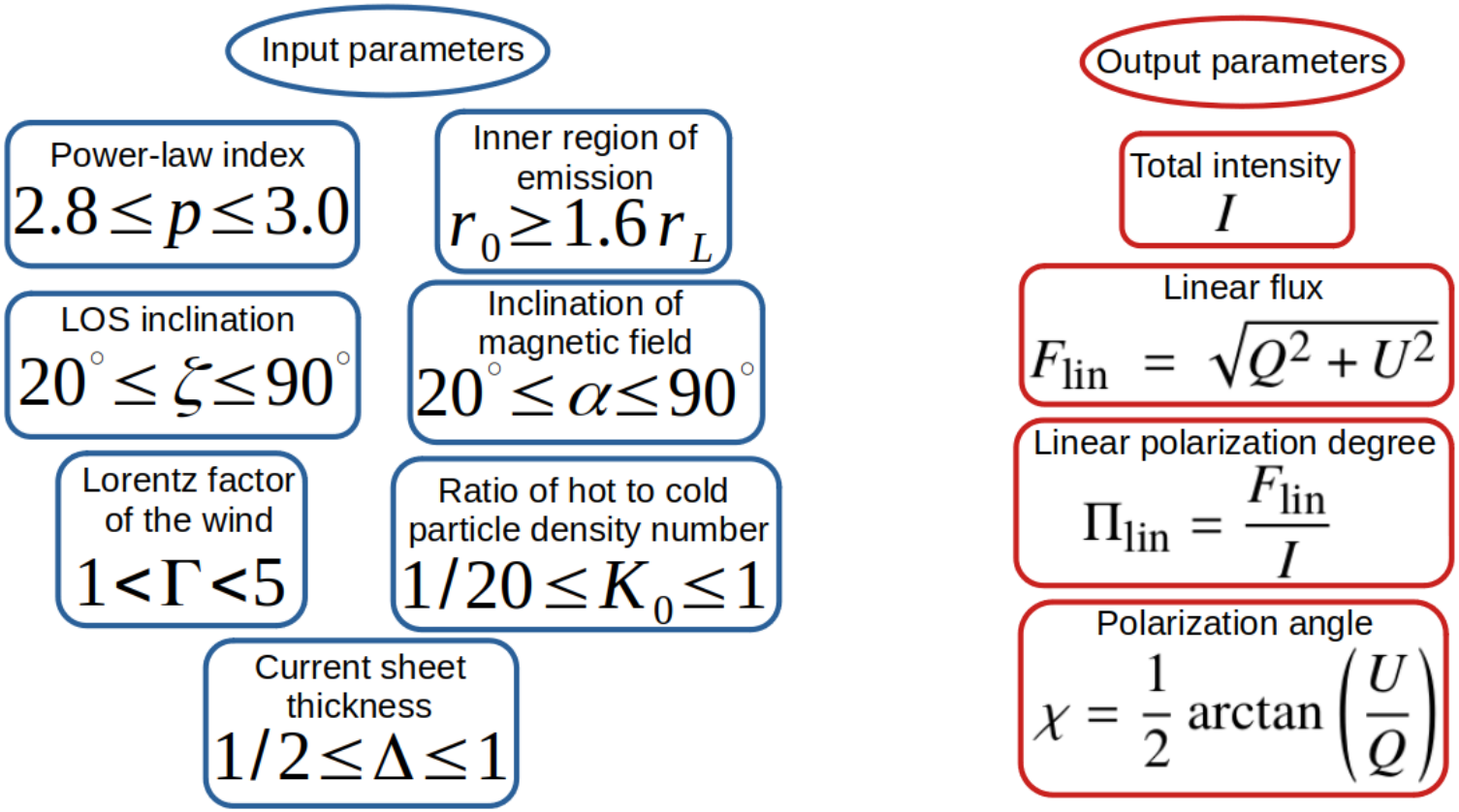

Figure: Description of the input parameters of the model.

Results

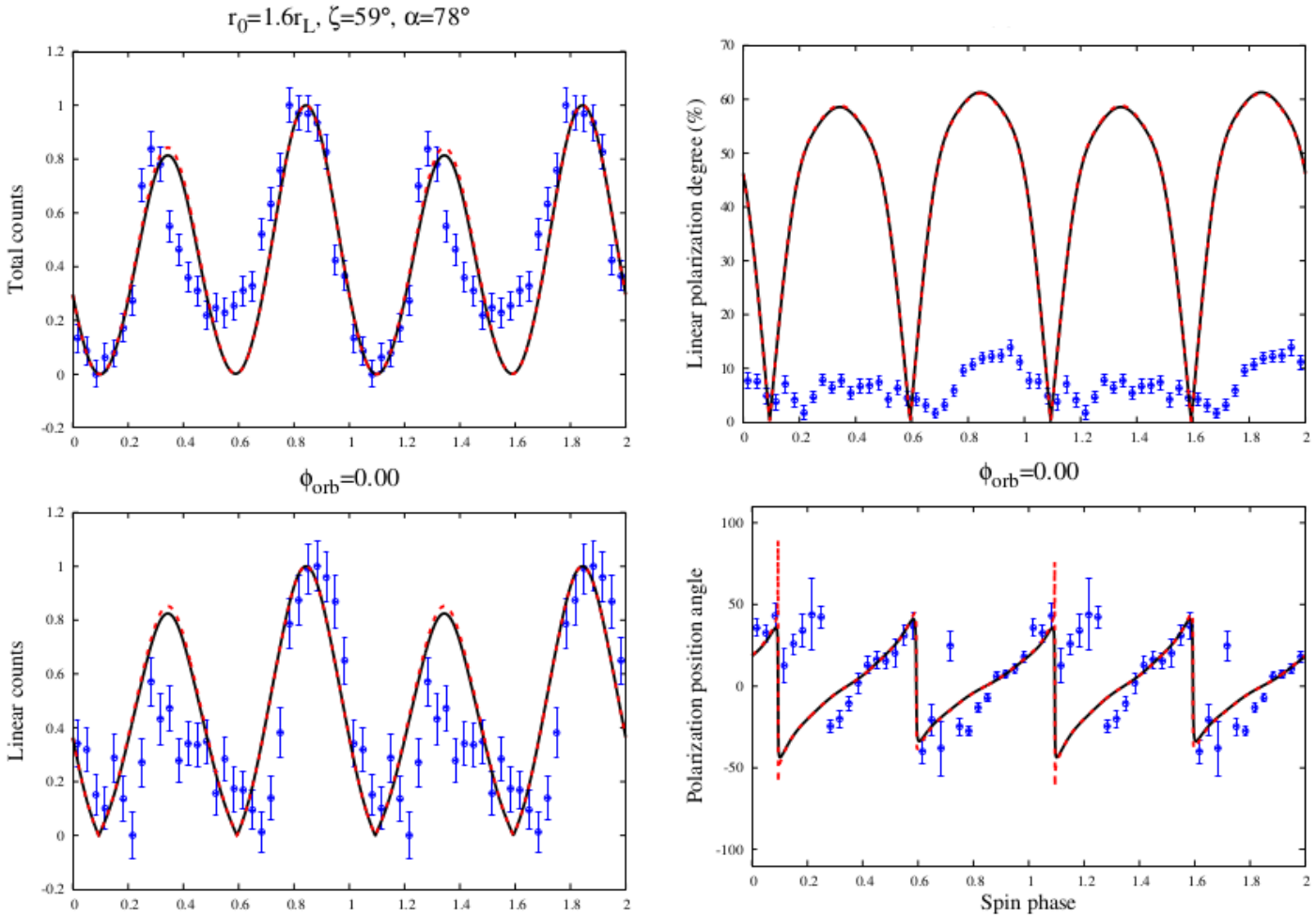

Figure: Best fit parameters at inferior conjunction $\Phi_{\rm orb} = 0.00$.
($p = 3, r_0 = 1.6 r_L, \zeta = 59°, \alpha = 78°, \Gamma = 1.2, K_0 = 1/20, \Delta \simeq 1$).
The red dashed lines correspond to $\alpha = 80°$.

Results

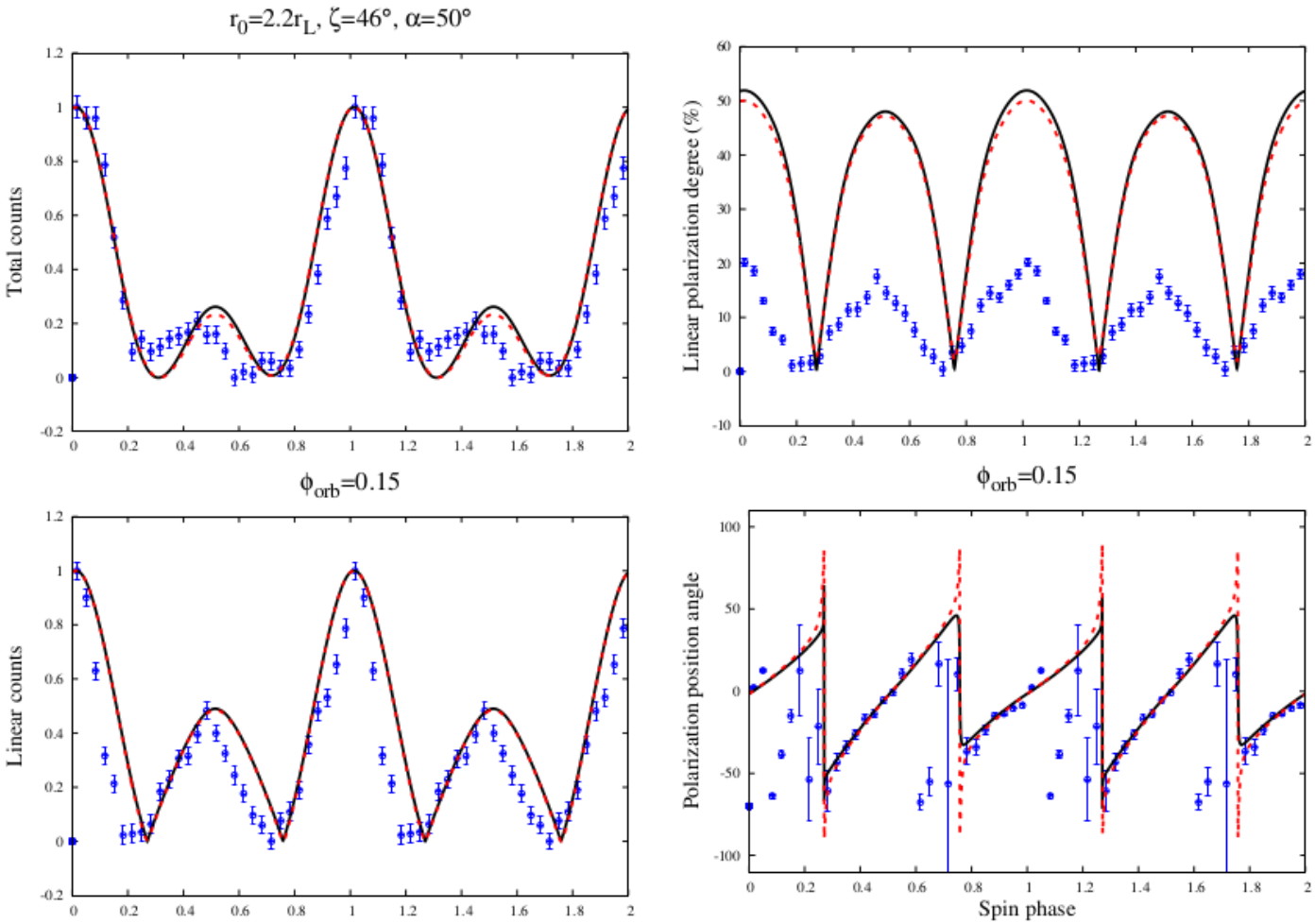

Figure: Best fit parameters at $\Phi_{\rm orb} = 0.15$.
($p = 3, r_0 = 2.2 r_L, \zeta = 46°, \alpha = 50°, \Gamma = 1.2, K_0 = 1/20, \Delta \simeq 1$).
The red dashed lines correspond to $\zeta = 44°$.

Conclusion

- Synchrotron emission origin: $r_0 \gtrsim 1.6 r_{\rm L}$

Conclusion

- Synchrotron emission origin: $r_0 \gtrsim 1.6 r_{\rm L}$
- At $\Phi_{\rm orb} = 0.00$: LOS inclination $\zeta = 59°$, obliquity $\alpha = 78°$.

Conclusion

- Synchrotron emission origin: $r_0 \gtrsim 1.6 r_{\rm L}$
- At $\Phi_{\rm orb} = 0.00$: LOS inclination $\zeta = 59°$, obliquity $\alpha = 78°$.
- RVM yields to $\zeta \simeq 60°$, obliquity $\alpha = 86°$ **(du Plessis et al. 2019)**

Conclusion

- Synchrotron emission origin: $r_0 \gtrsim 1.6 r_{\rm L}$
- At $\Phi_{\rm orb} = 0.00$: LOS inclination $\zeta = 59°$, obliquity $\alpha = 78°$.
- RVM yields to $\zeta \simeq 60°$, obliquity $\alpha = 86°$ **(du Plessis et al. 2019)**
- A model involving synchrotron emission at diametrically opposed regions gives $\zeta \simeq 60°$, obliquity $\alpha = 40°$ **(Potter and Buckley 2018)**

Conclusion

- Synchrotron emission origin: $r_0 \gtrsim 1.6 r_{\rm L}$
- At $\Phi_{\rm orb} = 0.00$: LOS inclination $\zeta = 59°$, obliquity $\alpha = 78°$.
- RVM yields to $\zeta \simeq 60°$, obliquity $\alpha = 86°$ **(du Plessis et al. 2019)**
- A model involving synchrotron emission at diametrically opposed regions gives $\zeta \simeq 60°$, obliquity $\alpha = 40°$ **(Potter and Buckley 2018)**
- A model of synchrotron emission produced at magnetic mirror points results in $50° \leq \zeta \leq 60°$ and $50° \leq \alpha \leq 60°$ **(Takata and Cheng 2019)**

Conclusion

- Synchrotron emission origin: $r_0 \gtrsim 1.6 r_{\rm L}$
- At $\Phi_{\rm orb} = 0.00$: LOS inclination $\zeta = 59°$, obliquity $\alpha = 78°$.
- RVM yields to $\zeta \simeq 60°$, obliquity $\alpha = 86°$ **(du Plessis et al. 2019)**
- A model involving synchrotron emission at diametrically opposed regions gives $\zeta \simeq 60°$, obliquity $\alpha = 40°$ **(Potter and Buckley 2018)**
- A model of synchrotron emission produced at magnetic mirror points results in $50° \leq \zeta \leq 60°$ and $50° \leq \alpha \leq 60°$ **(Takata and Cheng 2019)**
- Lorentz factor of wind $\Gamma \simeq 1.2$ yielding to 60% much smaller spin-down luminosity $L_{\rm sd} = 0.9 \times 10^{26}$ W compared to **Marsh et al. (2016)**

Conclusion

- Synchrotron emission origin: $r_0 \gtrsim 1.6 r_{\rm L}$
- At $\Phi_{\rm orb} = 0.00$: LOS inclination $\zeta = 59°$, obliquity $\alpha = 78°$.
- RVM yields to $\zeta \simeq 60°$, obliquity $\alpha = 86°$ **(du Plessis et al. 2019)**
- A model involving synchrotron emission at diametrically opposed regions gives $\zeta \simeq 60°$, obliquity $\alpha = 40°$ **(Potter and Buckley 2018)**
- A model of synchrotron emission produced at magnetic mirror points results in $50° \leq \zeta \leq 60°$ and $50° \leq \alpha \leq 60°$ **(Takata and Cheng 2019)**
- Lorentz factor of wind $\Gamma \simeq 1.2$ yielding to 60% much smaller spin-down luminosity $L_{\rm sd} = 0.9 \times 10^{26}$ W compared to **Marsh et al. (2016)**
- Density contrast between hot and cold plasmas $K_0 = 1/20$

Conclusion

- Synchrotron emission origin: $r_0 \gtrsim 1.6 r_{\rm L}$
- At $\Phi_{\rm orb} = 0.00$: LOS inclination $\zeta = 59°$, obliquity $\alpha = 78°$.
- RVM yields to $\zeta \simeq 60°$, obliquity $\alpha = 86°$ **(du Plessis et al. 2019)**
- A model involving synchrotron emission at diametrically opposed regions gives $\zeta \simeq 60°$, obliquity $\alpha = 40°$ **(Potter and Buckley 2018)**
- A model of synchrotron emission produced at magnetic mirror points results in $50° \leq \zeta \leq 60°$ and $50° \leq \alpha \leq 60°$ **(Takata and Cheng 2019)**
- Lorentz factor of wind $\Gamma \simeq 1.2$ yielding to 60% much smaller spin-down luminosity $L_{\rm sd} = 0.9 \times 10^{26}$ W compared to **Marsh et al. (2016)**
- Density contrast between hot and cold plasmas $K_0 = 1/20$
- Current sheet thickness $\Delta \lesssim 1$

Future work

Pre-whitening

Remove the contamination of the spin modulated pulsed emission

Fitting at the beat frequency

Fitting of the beat modulated polarized emission at different orbital phases

Binarity of AR Sco

Invoke the binarity characterizing AR Sco

Statistical modelling

Obtain a tight constraint on parameter space of AR Sco

Thank you for your attention!

Contact:

framamon@gmail.com